Article

Enantioconvergent Cu-catalysed *N*-alkylation of aliphatic amines

https://doi.org/10.1038/s41586-023-05950-8

Received: 12 September 2022

Accepted: 13 March 2023

Published online: 20 March 2023

Check for updates

Ji-Jun Chen[1,3], Jia-Heng Fang[1,3], Xuan-Yi Du[1,3], Jia-Yong Zhang[1], Jun-Qian Bian[1], Fu-Li Wang[1], Cheng Luan[2], Wei-Long Liu[1], Ji-Ren Liu[1], Xiao-Yang Dong[1], Zhong-Liang Li[2], Qiang-Shuai Gu[2], Zhe Dong[1] & Xin-Yuan Liu[1]✉

Chiral amines are commonly used in the pharmaceutical and agrochemical industries[1]. The strong demand for unnatural chiral amines has driven the development of catalytic asymmetric methods[1,2]. Although the *N*-alkylation of aliphatic amines with alkyl halides has been widely adopted for over 100 years, catalyst poisoning and unfettered reactivity have been preventing the development of a catalyst-controlled enantioselective version[3–5]. Here we report the use of chiral tridentate anionic ligands to enable the copper-catalysed chemoselective and enantioconvergent *N*-alkylation of aliphatic amines with α-carbonyl alkyl chlorides. This method can directly convert feedstock chemicals, including ammonia and pharmaceutically relevant amines, into unnatural chiral α-amino amides under mild and robust conditions. Excellent enantioselectivity and functional-group tolerance were observed. The power of the method is demonstrated in a number of complex settings, including late-stage functionalization and in the expedited synthesis of diverse amine drug molecules. The current method indicates that multidentate anionic ligands are a general solution for overcoming transition-metal-catalyst poisoning.

α-Chiral aliphatic amines are common chiral synthons and catalysts for the asymmetric synthesis of natural products, pharmaceuticals, agrochemicals and functional materials[1,2]. Consequently, the quest for their efficient and practical preparation has promoted the revolution of catalytic enantioselective synthesis. The first chiral transition-metal catalysis developed by Knowles was to synthesize unnatural α-amino acid[6]. The strong demand for chiral amines has encouraged the establishment of numerous catalytic asymmetric synthesis strategies, including asymmetric hydrogenation[7], nucleophilic addition to imines[8], alkene hydroamination[9,10], carbene and nitrene insertion[11,12], allylic and propargylic amination[13–15] and so on, both on the laboratory scale and in industrial processes. In this regard, primary and secondary aliphatic amines are among the most purchasable building blocks[16], and some of them, as well as ammonia, are also bulk industrial feedstocks[17,18]. Current asymmetric catalysis for *N*-alkylation of these amines usually takes advantage of the imine–enamine chemistry, generating an α-carbon chiral centre from the corresponding sp^2 carbon (Fig. 1a, left). By contrast, the corresponding *N*-alkylation with desired sp^3-alkyl fragments via direct C–N bond formation is a more straightforward disconnection, which once achieved would constitute a conceptually simple and practically appealing strategy for expediently preparing structurally divergent α-chiral aliphatic amines. Nevertheless, it has so far remained relatively underdeveloped[12,14,19].

In this aspect, the *N*-alkylation of amines with alkyl halides discovered by Hofmann in 1850 was the most straightforward and well adopted method[3,4] (Fig. 1a, right), owing to the readily available starting materials and their prevailing use in both industrial and academic settings[20]. However, the asymmetric version of this reaction has thus far largely relied on the use of enantioenriched alkyl halides, of which the stereoselective synthesis may be arduous. As for more readily available racemic alkyl halides, chiral transition-metal catalysis[21,22] is highly promising for delivering the enantioconvergent *N*-alkylation, yet has so far been unreported for aliphatic amines and ammonia. Major obstacles in this aspect include: the high Lewis basicity of aliphatic amines and ammonia that probably leads to transition-metal-catalyst poisoning[5]; and the selective deprotonation of the weakly acidic N–H bonds of these amines without non-stereoselective *N*-alkylation in the presence of alkyl halides[23]. Accordingly, known transition-metal-catalysed enantioconvergent *N*-alkylation with racemic alkyl halides has been limited to aryl amines or ammonia surrogates with diminished Lewis basicity and enhanced N–H acidity[24–30]. In particular, Fu, Peters and their co-workers have pioneered the copper-catalysed enantioconvergent amination of racemic alkyl halides under photochemical conditions[24,26–28] and have recently extended the chemistry to primary carboxamides[26]. We have also reported copper(I)/*N*,*N*,*P*-ligand catalysts for similar amination using sulfoximines[29]. All these methods suffer from multistep deprotection and alkylation manipulations to access α-chiral aliphatic amines, which limits the real-world applications in medicinal chemistry. As such, a practical one-step enantioconvergent *N*-alkylation of aliphatic amines and ammonia would fit the strong synthetic demand for chiral

[1]Shenzhen Grubbs Institute and Department of Chemistry, Guangdong Provincial Key Laboratory of Catalysis, Southern University of Science and Technology, Shenzhen, China. [2]Academy for Advanced Interdisciplinary Studies and Department of Chemistry, Southern University of Science and Technology, Shenzhen, China. [3]These authors contributed equally: Ji-Jun Chen, Jia-Heng Fang, Xuan-Yi Du. ✉e-mail: liuxy3@sustech.edu.cn

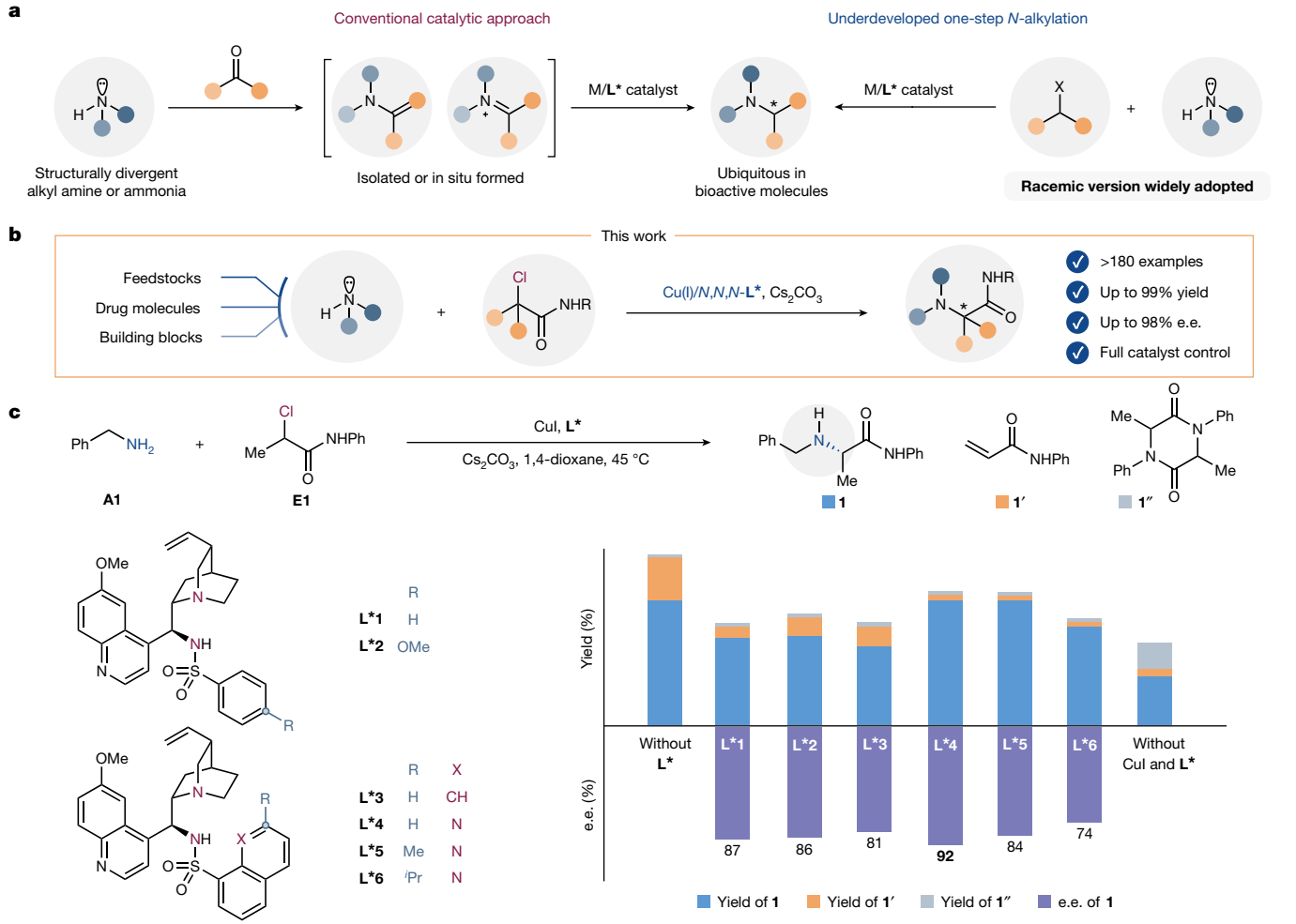

Fig. 1 | Challenges and development of enantioconvergent *N*-alkylation of aliphatic amines and ammonia for the synthesis of α-chiral aliphatic amines. a, α-Chiral aliphatic amines are usually synthesized from corresponding sp^2 fragments; asymmetric coupling with sp^3 fragments is underdeveloped. **b**, Copper-catalysed enantioconvergent alkylation of aliphatic amines and ammonia to directly access unnatural α-amino amides. **c**, Reaction development. See Supplementary Tables 4 and 8 for detailed information. M, metal; Me, methyl; ^{i}Pr, isopropyl.

aliphatic amines in both academic research and the pharmaceutical industry.

To overcome the aforementioned difficulties and given the great application potential, we envisaged that finely tuned chiral multidentate anionic ligands[31,32] with strong binding affinities to metal catalysts would not only overcome the catalyst poisoning by aliphatic amines or ammonia but also elicit high chemoselectivity and enantioselectivity. Here we disclose our efforts in developing a series of chiral multidentate anionic *N*,*N*,*N*-ligands that enable a general and practical copper-catalysed enantioconvergent *N*-alkylation under operationally simple and mild thermal conditions (Fig. 1b). The reaction successfully accommodates a diverse range of aliphatic amines (>100 examples) that are readily available industrial feedstocks, drug molecules or building blocks, and even tolerates, although partially, the most challenging, ammonia. In addition, the use of highly transformable secondary as well as tertiary α-carbonyl alkyl chlorides as the alkylation reagents further strengthens the synthetic potential of this methodology. Accordingly, the reaction provides facile access to a large number of α-chiral aliphatic amines (>180 examples) in moderate to high yield with high catalyst-controlled stereoselectivity. The integration of this reaction with additional one- or two-step transformations leads to the expedient preparation of six hybrid drugs, the straightforward late-stage C(sp^3)–H functionalization of two natural products and one drug, and the shortened catalytic enantioselective synthesis of one commercial drug. The preliminary mechanistic results support the multidentate coordination of these *N*,*N*,*N*-ligands to copper and the likely outer-sphere amine attack for the C–N bond formation.

We first investigated the enantioconvergent *N*-alkylation reaction of benzylamine **A1** with racemic α-carbonyl alkyl chloride **E1** (Fig. 1c), considering that enantioenriched unnatural α-amino acid derivatives have widespread use in a variety of fields such as organic synthesis as well as biological, pharmaceutical and material sciences[33]. After screening several parameters of the reaction (Supplementary Tables 1–4), we found the use of our previous copper catalyst with cinchona alkaloid-derived bidentate anionic sulfonamide ligand **L*1** (ref. 34) successfully led to the desired product **1** in 68% yield with 87% enantiomeric excess (e.e.) (Fig. 1c). In addition, we also observed the minor formation of common elimination and self-dimerization side products **1′** and **1″**, respectively, albeit with low yield. Changing the phenyl group of the sulfonamide moiety in **L*1** to a *para*-methoxyphenyl or a 1-naphthyl group in **L*2** or **L*3**, respectively, did not provide any obvious improvement in either chemoselectivity or enantioselectivity. We speculated that the moderate reaction efficiency and non-ideal stereoselectivity might indicate the occurrence of catalyst poisoning to a certain extent. Accordingly, we next installed an additional coordination site by switching the 1-naphthyl group in **L*3** to an 8-quinolinyl group in **L*4**, which we expected would further tighten the ligand binding. Indeed, **L*4** delivered a substantially enhanced yield of the desired

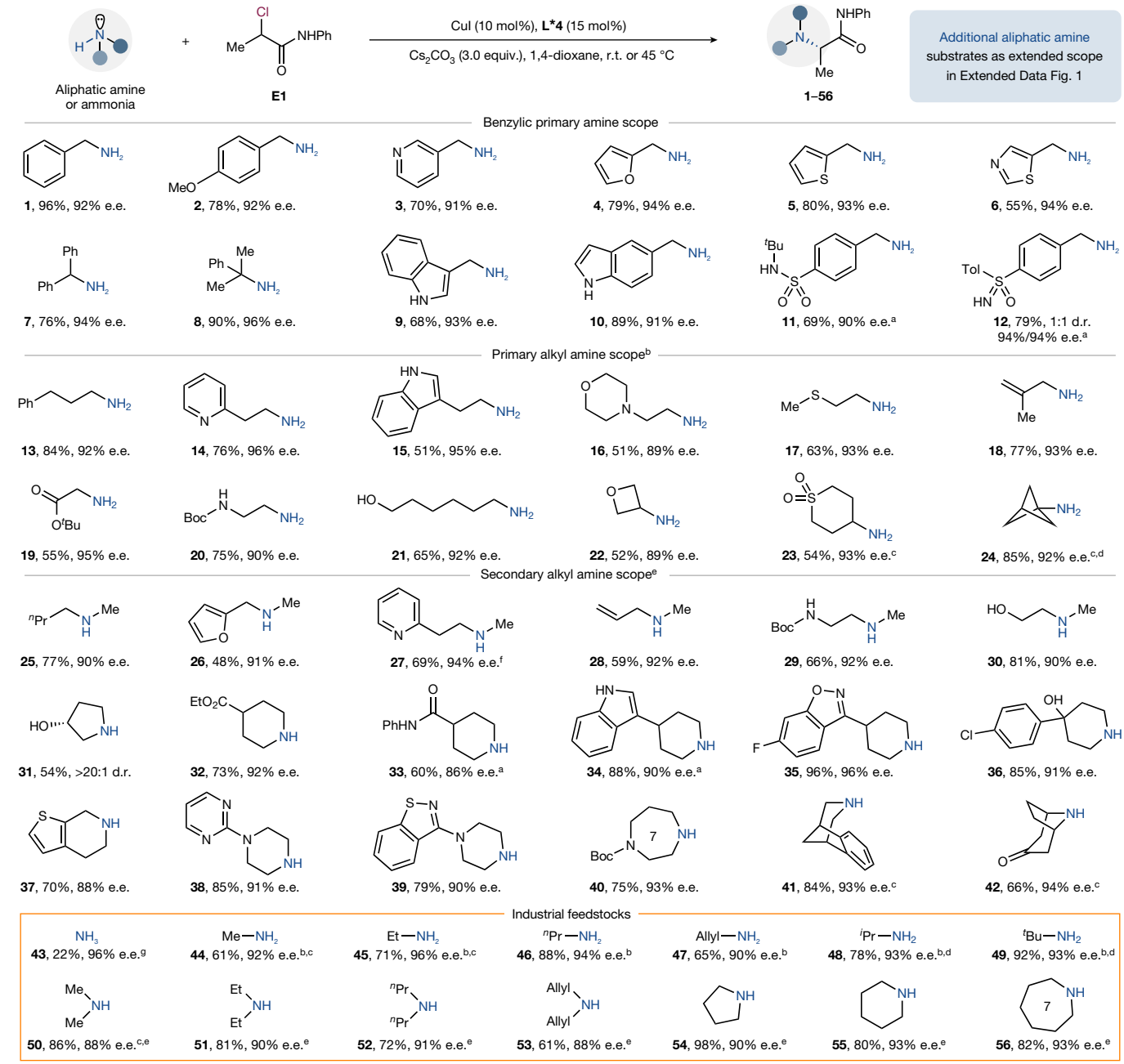

Fig. 2 | Substrate scope of amines. Standard reaction conditions: amine (0.20 mmol), racemic alkyl chloride **E1** (1.5 equiv.), CuI (10 mol%), **L*4** (15 mol%) and Cs_2CO_3 (3.0 equiv.) in 1,4-dioxane (4.0 ml) under argon at 45 °C. The yields are isolated. The e.e. values are based on chiral high-performance liquid chromatography analysis. The diastereomeric ratio (d.r.) value is based on crude ^{1}H NMR analysis. [a]Cs_2CO_3 (4.0 equiv.). [b]**L*5** (15 mol%) in *N*-methyl-2-pyrrolidone/ethyl acetate (2.4 ml/1.6 ml) at room temperature (r.t.). [c]Amine hydrochloride (0.20 mmol) and Cs_2CO_3 (4.0 equiv.). [d]**L*4** (15 mol%). [e]$CuBH_4(PPh_3)_2$ (10 mol%), and **L*5** (15 mol%) in *N*,*N*-dimethylformamide/cyclohexane (3.2 ml/0.8 ml) at r.t. [f]Amine dihydrochloride (0.20 mmol) and Cs_2CO_3 (5.0 equiv.). [g]Ammonia (10 equiv.), racemic alkyl chloride **E1** (0.20 mmol) and Cs_2CO_3 (10 equiv.) in cyclohexane (2.0 ml) at r.t. Additional aliphatic amine substrate scope is presented in Extended Data Fig. 1. Boc, *tert*-butoxycarbonyl; Et, ethyl; ^{n}Pr, *n*-propyl; Ph, phenyl; ^{t}Bu, *tert*-butyl; Tol, tolyl.

product **1** together with slightly boosted e.e. Remarkably, the catalyst from **L*4**, once formed in situ, retained its catalytic activity in three runs of consecutive reactions over more than one week (Supplementary Fig. 1). In addition, only marginal ligand displacement was observed when the preformed complex from **L*4** was exposed to up to 100 equiv. of aliphatic amines at 80 °C for 0.5 h (Supplementary Fig. 2). These results clearly evidenced the strong coordination capability of such *N*,*N*,*N*-ligands. Using *ortho*-substituents to partially discourage the quinoline binding led to diminished e.e. (**L*5** and **L*6**) and yield (**L*6**), thus lending support to the importance of the presumed tridentate binding mode. Accordingly, the optimal conditions (for results of additional reaction condition variations, see Supplementary Tables 5–7) for the enantioconvergent *N*-alkylation reaction were as follows: **A1** reacted with 1.5 equiv. of **E1** in the presence of 10 mol% copper iodide (CuI), 15 mol% **L*4** and 3.0 equiv. of caesium carbonate (Cs_2CO_3) in 1,4-dioxane (0.05 M) at 45 °C for 72 h under argon, affording **1** in 98% yield with 92% e.e. Further control experiments indicated that the base additive Cs_2CO_3 alone (without CuI and **L***, where **L*** is a chiral ligand) was able to elicit the considerable formation of *N*-alkylation product **1** together with side product **1″**. The sole addition of **L*4** did not affect the

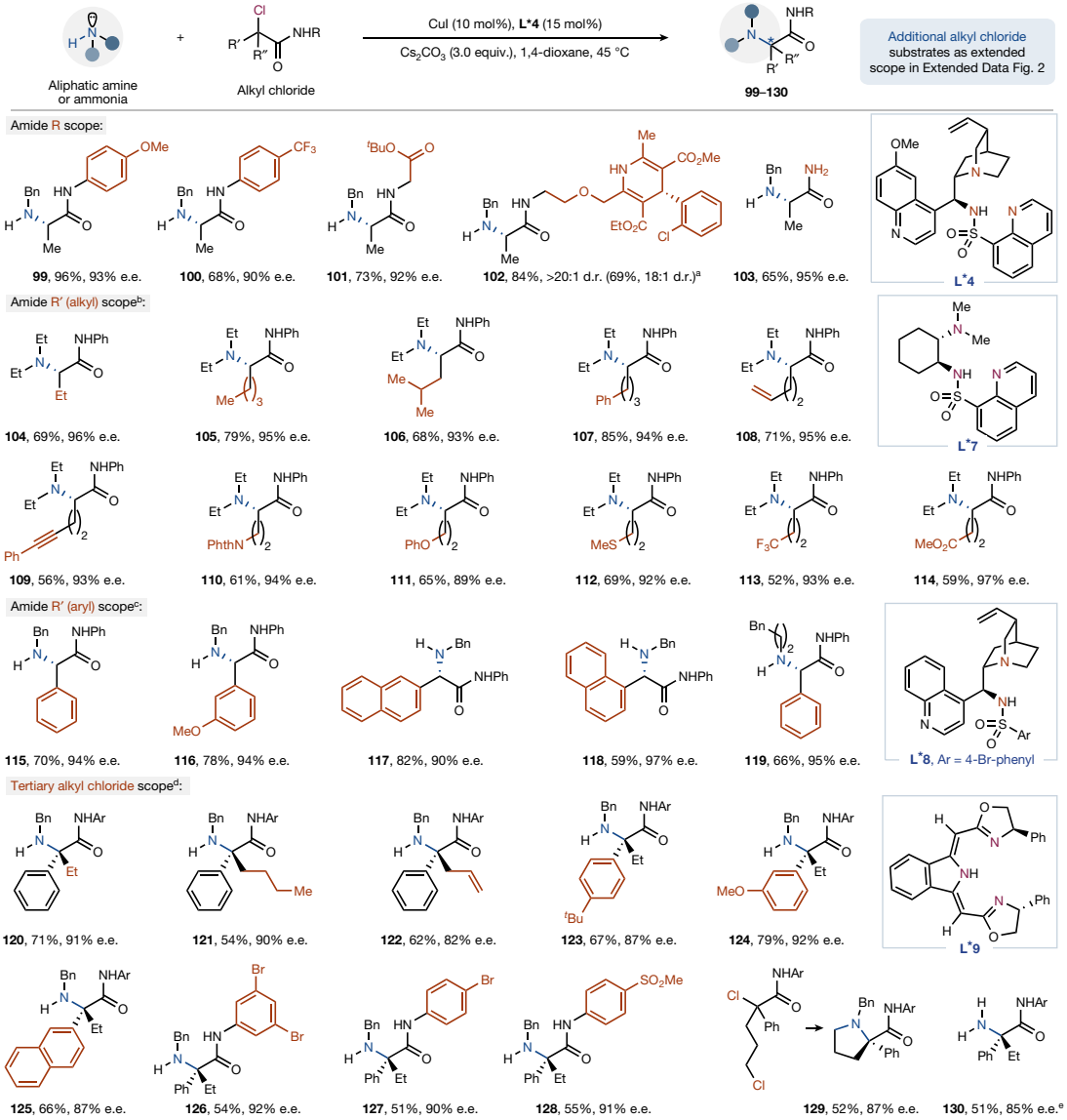

Fig. 3 | Substrate scope of α-carbonyl alkyl chlorides. Standard reaction conditions: amine (0.20 mmol), racemic alkyl chloride (1.5 equiv.), CuI (10 mol%), **L*4** (15 mol%) and Cs_2CO_3 (3.0 equiv.) in 1,4-dioxane (4.0 ml) under argon at 45 °C. The yields are isolated. The e.e. values are based on chiral high-performance liquid chromatography analysis. The diastereomeric (d.r.) value is based on crude ^{1}H NMR analysis. [a]Racemic alkyl chloride (1.0 equiv.). [b]**L*7** (15 mol%) in benzene (4.0 ml) at 50 °C. [c]CuSCN (10 mol%), **L*8** (15 mol%) in tetrahydrofuran (4.0 ml) at r.t. [d]Amine (1.2 equiv.), racemic alkyl chloride (0.20 mmol), CuBr·SMe_2 (10 mol%), **L*9** (15 mol%) and K_3PO_4/Cs_2CO_3 (3.0 equiv/0.20 equiv.) in methyl *tert*-butyl ether (2.0 ml) at r.t. Ar, 3,5-$(CF_3)_2$Ph. [e]$CuBH_4(PPh_3)_2$ (10 mol%) and ammonia (3.0 equiv.) in Et_2O (4.0 ml). Additional alkyl chloride substrate scope is presented in Extended Data Fig. 2. Bn, benzyl.

base-induced background reaction (Supplementary Table 8, entry 3) whereas that of CuI remarkably enhanced the *N*-alkylation with the selective formation of the other side product **1′**. These results together emphasized the combined striking effects of CuI and **L*4** in tuning the chemoselectivity and enantioselectivity of this *N*-alkylation reaction. In addition, we were able to prepare the typical ligand **L*4** in tens of grams in one single batch from commercially available starting materials and directly employed the crude ligand in the enantioselective *N*-alkylation reaction without erosion of the overall performance (Supplementary Fig. 3). Furthermore, the *N*-alkylation reaction at the gram scale (Supplementary Fig. 4) showed comparable efficiency and enantioselectivity.

Concerning the substrate scope, we first surveyed readily available amine building blocks (Fig. 2; see Extended Data Fig. 1 for additional examples). We found that primary and secondary aliphatic amines could be alkylated under very similar reaction conditions to yield α-amino amide products (**1**–**42**) with high enantioselectivity (for detailed discussions, see Extended Data Fig. 4; for additional condition optimization, see Supplementary Tables 9–14). Perhaps more importantly, this transformation has excellent functional-group tolerance and chemoselectivity. Pharmaceutically important motifs[35], including pyridine (**3**), thiophene (**5**), thiazole (**6**), alkylsulfide (**17**), oxetane (**22**), [1,1,1]-bicyclopentane (**24**), allylamine (**28**), benzo[*d*]isoxazole (**35**), pyrimidine (**38**), benzo[*d*]isothiazole (**39**) and alkyl ketone (**42**), were all successfully coupled. In the presence of free indole (**9, 10** and **15**), sulfonamide (**11**), sulfoximine (**12**), carbamate (**20**) and alcohol (primary, **21**; secondary, **31**; tertiary, **36**), alkyl amines were preferentially coupled with the high enantioselectivity being untouched (for unsuccessful examples, see Supplementary Fig. 5). We ascribed this unique chemoselectivity to a likely outer-sphere amine-attack mechanism for the C–N bond formation (see the mechanistic section below for detailed discussions).

Next, we switched our efforts to amines that are bulk industrial feedstocks[17,18]. Among others, ammonia, methylamine and dimethylamine are of particular interest owing to their substantially high

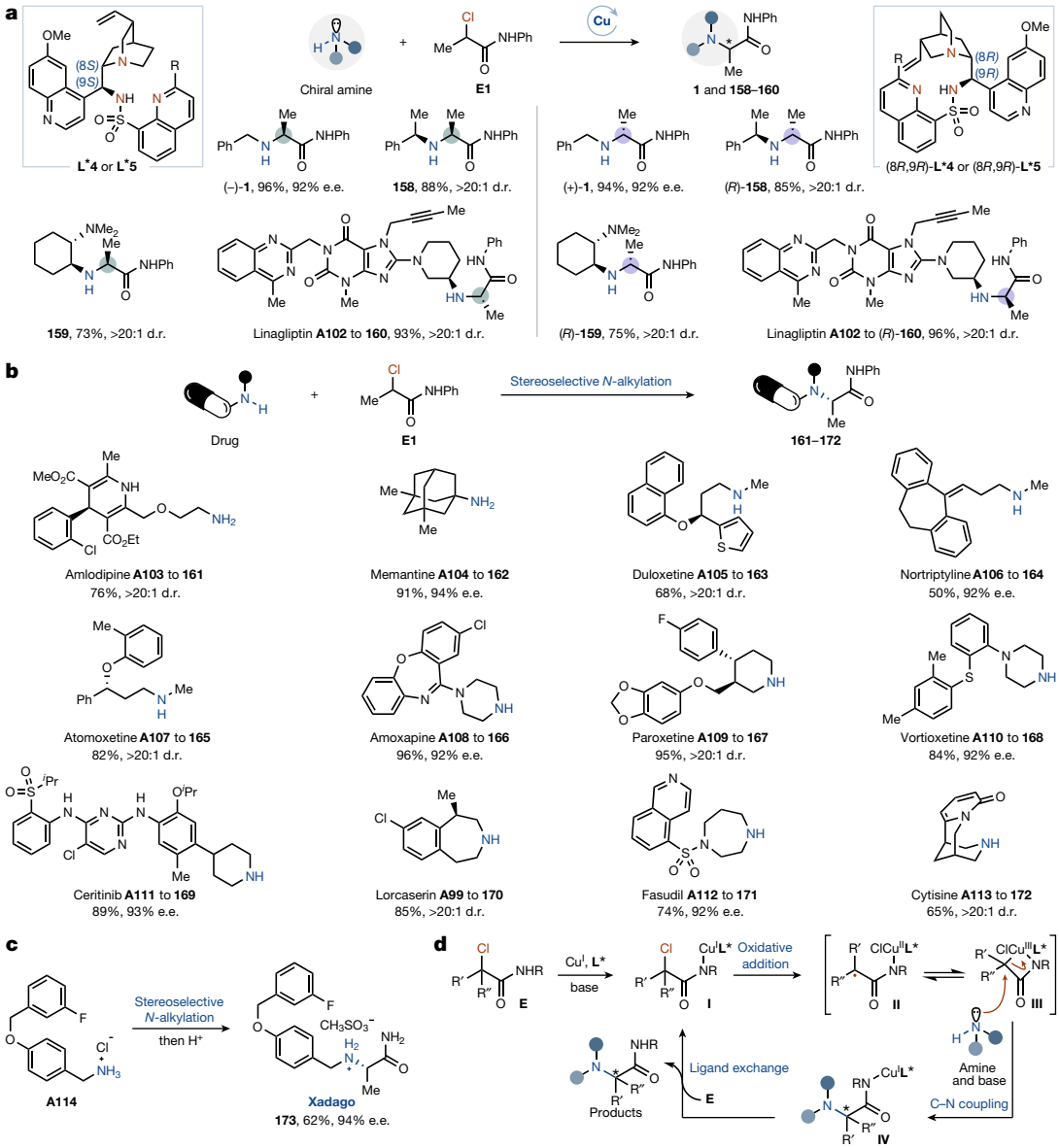

Fig. 4 | Synthetic applications and proposed mechanism. a, The reaction showed high levels of catalyst-controlled stereoselectivity when alkylating chiral aliphatic amines. **b**, The reaction readily accommodated a range of complex drug molecules featuring aliphatic amine functionalities. **c**, The enantioselective *N*-alkylation reaction led to an expedited synthesis of the drug Xadago. **d**, The proposed mechanism features a likely direct outer-sphere amine attack of intermediate **III** for the C–N bond formation, which readily distinguishes this reaction from known transition-metal-catalysed enantioconvergent C–N cross-coupling methods.

annual outputs[17,18] and notorious catalyst-poisoning capability[5]. Fortunately, our catalyst system remains fully compatible with methylamine and dimethylamine, leading to **44** and **50** in moderate to high yield with high e.e. More importantly, the catalyst even provides remarkably high enantioselectivity for the *N*-alkylation of ammonia to **43**. Nonetheless, the yield of product **43** was low, probably owing to the relatively weak nucleophilicity of ammonia (for side products, see Supplementary Table 15; for additional examples, see Supplementary Fig. 5), which is currently under further development. In addition, a panel of other amine feedstocks, particularly those acyclic secondary amines, all smoothly underwent the *N*-alkylation reaction. Notably, as many amines are commercially available as hydrochloride salts, we have adapted our conditions for their direct use in the process (for example, **24** and **27**), thereby avoiding cumbersome deprotection.

In regards to the scope of the alkylation reagents (Fig. 3; see Extended Data Fig. 2 for additional examples), we found that α-chloro secondary amides bearing various *N*-substituents (**99**–**103**) or α-alkyl (**104**–**114**) or α-aryl groups (**115**–**119**) readily underwent the amination reaction with high efficiency and selectivity. However, owing to the distinct steric natures of different alkyl electrophiles, the steric properties of chiral ligands needed to be tuned correspondingly to balance reactivity and selectivity (for detailed discussions, see Extended Data Fig. 4; for additional condition optimization, see Supplementary Tables 16–21). In addition, α-carbonyl tertiary alkyl chlorides furnished the desired *N*-alkyl products **120**–**128** with good yield and excellent enantioselectivity (for detailed condition optimization, see Supplementary Table 22). Interestingly, a tertiary alkyl chloride bearing an additional primary chloride functional group directly yielded an unnatural proline analogue **129**. Last, but not least, ammonia was alkylated under slightly modified conditions to give free primary amine **130** with good yield and enantioselectivity (Supplementary Table 23). Notably, these α-tetrasubstituted α-amino amides are robust building blocks for unnatural peptide synthesis.

Given the heavy presence of primary and secondary chiral aliphatic amines in pharmaceuticals (44 among the top 200 small molecule pharmaceuticals in 2021)[36], we wondered whether our tridentate ligands and their pseudo-enantiomers could override the stereoselectivity induced by the pre-existing stereocentres in these chiral amine substrates to achieve full catalyst control. We found that **L*4** and its (8*R*,9*R*)-pseudo-enantiomer gave two C2-diastereoisomers of **158**, respectively, with higher than 20:1 selectivity (Fig. 4a). For simple benzylamine, (8*R*,9*R*)-**L*4** led to (+)–**1** with exactly the same enantioselectivity. In addition, **L*5** and its (8*R*,9*R*)-pseudo-enantiomer also showed highly catalyst-controlled stereoselectivity, particularly on the complex drug molecule linagliptin **A102**. These results clearly demonstrate that this method would have broad application in stereochemically complex molecule synthesis.

We then investigated the direct *N*-alkylation of a panel of additional 12 drugs or bioactive molecules under our reaction conditions. Despite their very complex structures with greatly distinct steric and stereochemical properties, we generally observed (**161**–**172** in Fig. 4b) good to excellent reaction efficiency with high stereoselectivity as well as high integrity of pre-existing functional groups and stereocentres. The ready access to α-chloro secondary amides via facile α-chlorination and/or amide bond formation also allowed us to quickly increase the molecular complexity by forming new chiral C–N bonds (hybrid drugs[37], see Extended Data Fig. 3a; natural product late-stage C(sp^3)–H functionalization, see Extended Data Fig. 3b).

This *N*-alkylation reaction also enabled the catalytic enantioselective synthesis of the anti-Parkinson drug Xadago (**173**) in as few as two steps (Fig. 4c)[38]. As mentioned above, the synthetic potential of this *N*-alkylation reaction is further enhanced by the presence of a readily transformable carboxamide moiety in the product. We briefly examined this point by converting it to an amine or an alcohol (Extended Data Fig. 3c,d), during which we did not observe any loss of enantiopurity. These results highlight the synthetic practicality of this methodology.

The X-ray crystallographic analysis of one Cu(II) complex with **L*7** revealed the tridentate binding mode of this *N*,*N*,*N*-ligand (Extended Data Fig. 5a and Supplementary Fig. 9). Further control experiments using this Cu(II) complex indicated comparable catalytic activity to that of the catalyst generated in situ (Extended Data Fig. 5b). In addition, a linear relationship between the catalyst and product e.e. values was observed, indicating a likely 1:1 copper-to-ligand ratio in the enantiodiscrimination reaction complex (Supplementary Fig. 10). All these results supported the mononuclear copper species coordinated with one chiral ligand as the active intermediates in the reaction. Subsequent electron paramagnetic resonance and high-resolution mass spectroscopy analyses of the reaction mixture suggested the likely formation of alkyl radicals (Extended Data Fig. 5c), which was further supported by the radical clock experiment (Extended Data Fig. 5d). Additional control experiments indicated the likely formation of alkyl radicals in the absence of amines under the otherwise standard conditions (Extended Data Fig. 5e,f). These results collectively suggested a dispensable role of amines in the activation of alkyl chlorides by the copper catalyst. Importantly, the dual nucleophilic substrate bearing aliphatic amine and sulfoximine functionalities underwent highly chemoselective amine *N*-alkylation and sulfoximine C–N cross-coupling under the current and our previously reported conditions[29] (Extended Data Fig. 5g; see Supplementary Fig. 11 for additional results), respectively. These results strongly suggested a very different mechanism of the current enantioselective *N*-alkylation from that of known transition-metal-catalysed enantioconvergent C–N cross-coupling reactions[24–29].

On the basis of these experimental results, we proposed a reaction mechanism, as shown in Fig. 4d. The reaction starts with the formation of cuprate intermediate **I** (for results supporting this step, see Supplementary Figs. 12–18), of which the intramolecular oxidative addition gives rise to **II** and **III** in equilibrium. The subsequent direct outer-sphere amine attack of **III** in the presence of base delivered **IV** (for a brief discussion on the enantiodifferentiation based on this reaction mechanism, see Supplementary Fig. 19), of which the ligand exchange with alkyl chloride **E** releases the enantioenriched *N*-alkylation product and regenerates intermediate **I**, closing the catalytic cycle. The key outer-sphere amine attack was supported by the aforementioned failed *N*-alkylation of sulfoximines given their inherently low nucleophilicity. In addition, aliphatic amines of remarkably different steric (for examples, see the results of **1, 7** and **8** in Fig. 2) and stereochemical (for examples, see the results of **158**–**160** in Fig. 4) properties delivered almost the same enantioselectivity.

Online content

Any methods, additional references, Nature Portfolio reporting summaries, source data, extended data, supplementary information, acknowledgements, peer review information; details of author contributions and competing interests; and statements of data and code availability are available at https://doi.org/10.1038/s41586-023-05950-8.

1. Ricci, A. & Bernardi, L. (eds) *Methodologies in Amine Synthesis: Challenges and Applications* (Wiley, 2021).
2. Nugent, T. C. (ed.) *Chiral Amine Synthesis: Methods, Developments and Applications* (Wiley, 2010).
3. von Hofmann, A. W. V. Researches regarding the molecular constitution of the volatile organic bases. *Phil. Trans. R. Soc. Lond.* **140**, 93–131 (1850).
4. McMurry, J. *Organic Chemistry* 799 (Cengage Learning, 2016).
5. Kwan, M. H. T. et al. Deactivation mechanisms of iodo-iridium catalysts in chiral amine racemization. *Tetrahedron* **80**, 131823 (2021).
6. Knowles, W. S., Sabacky, M. J. & Vineyard, B. D. Catalytic asymmetric hydrogenation. *J. Chem. Soc. Chem. Commun.* **1972**, 10–11 (1972).
7. Cabré, A., Verdaguer, X. & Riera, A. Recent advances in the enantioselective synthesis of chiral amines via transition metal-catalyzed asymmetric hydrogenation. *Chem. Rev.* **122**, 269–339 (2022).
8. Kobayashi, S., Mori, Y., Fossey, J. S. & Salter, M. M. Catalytic enantioselective formation of C–C bonds by addition to imines and hydrazones: a ten-year update. *Chem. Rev.* **111**, 2626–2704 (2011).
9. Shi, S.-L., Wong, Z. L. & Buchwald, S. L. Copper-catalysed enantioselective stereodivergent synthesis of amino alcohols. *Nature* **532**, 353–356 (2016).
10. Xi, Y., Ma, S. & Hartwig, J. F. Catalytic asymmetric addition of an amine N–H bond across internal alkenes. *Nature* **588**, 254–260 (2020).
11. Davies, H. M. L. & Manning, J. R. Catalytic C–H functionalization by metal carbenoid and nitrenoid insertion. *Nature* **451**, 417–424 (2008).
12. Li, M.-L., Yu, J.-H., Li, Y.-H., Zhu, S.-F. & Zhou, Q.-L. Highly enantioselective carbene insertion into N–H bonds of aliphatic amines. *Science* **366**, 990–994 (2019).
13. Rössler, S. L., Petrone, D. A. & Carreira, E. M. Iridium-catalyzed asymmetric synthesis of functionally rich molecules enabled by (phosphoramidite,olefin) ligands. *Acc. Chem. Res.* **52**, 2657–2672 (2019).
14. Hartwig, J. F. & Stanley, L. M. Mechanistically driven development of iridium catalysts for asymmetric allylic substitution. *Acc. Chem. Res.* **43**, 1461–1475 (2010).
15. Lauder, K., Toscani, A., Scalacci, N. & Castagnolo, D. Synthesis and reactivity of propargylamines in organic chemistry. *Chem. Rev.* **117**, 14091–14200 (2017).
16. Wang, Y., Haight, I., Gupta, R. & Vasudevan, A. What is in our kit? An analysis of building blocks used in medicinal chemistry parallel libraries. *J. Med. Chem.* **64**, 17115–17122 (2021).
17. Pattabathula, V. in *Kirk-Othmer Encyclopedia of Chemical Technology* https://doi.org/j8cr (Wiley, 2019).
18. Roose, P. & Turcotte, M. G. in *Kirk-Othmer Encyclopedia of Chemical Technology* https://doi.org/j8cq (Wiley, 2016).
19. Thorpe, T. W. et al. Multifunctional biocatalyst for conjugate reduction and reductive amination. *Nature* **604**, 86–91 (2022).
20. Brown, D. G. & Boström, J. Analysis of past and present synthetic methodologies on medicinal chemistry: where have all the new reactions gone? *J. Med. Chem.* **59**, 4443–4458 (2016).
21. Cherney, A. H., Kadunce, N. T. & Reisman, S. E. Enantioselective and enantiospecific transition-metal-catalyzed cross-coupling reactions of organometallic reagents to construct C–C bonds. *Chem. Rev.* **115**, 9587–9652 (2015).
22. Choi, J. & Fu, G. C. Transition metal-catalyzed alkyl–alkyl bond formation: another dimension in cross-coupling chemistry. *Science* **356**, eaaf7230 (2017).
23. Kim, H., Heo, J., Kim, J., Baik, M.-H. & Chang, S. Copper-mediated amination of aryl C–H bonds with the direct use of aqueous ammonia via a disproportionation pathway. *J. Am. Chem. Soc.* **140**, 14350–14356 (2018).
24. Kainz, Q. M. et al. Asymmetric copper-catalyzed C–N cross-couplings induced by visible light. *Science* **351**, 681–684 (2016).
25. Bartoszewicz, A., Matier, C. D. & Fu, G. C. Enantioconvergent alkylations of amines by alkyl electrophiles: copper-catalyzed nucleophilic substitutions of racemic α-halolactams by indoles. *J. Am. Chem. Soc.* **141**, 14864–14869 (2019).
26. Chen, C., Peters, J. C. & Fu, G. C. Photoinduced copper-catalysed asymmetric amidation via ligand cooperativity. *Nature* **596**, 250–256 (2021).

27. Cho, H., Suematsu, H., Oyala, P. H., Peters, J. C. & Fu, G. C. Photoinduced, copper-catalyzed enantioconvergent alkylations of anilines by racemic tertiary electrophiles: synthesis and mechanism. *J. Am. Chem. Soc.* **144**, 4550–4558 (2022).
28. Lee, H. et al. Investigation of the C–N bond-forming step in a photoinduced, copper-catalyzed enantioconvergent N-alkylation: characterization and application of a stabilized organic radical as a mechanistic probe. *J. Am. Chem. Soc.* **144**, 4114–4123 (2022).
29. Zhang, Y.-F. et al. Enantioconvergent Cu-catalyzed radical C–N coupling of racemic secondary alkyl halides to access α-chiral primary amines. *J. Am. Chem. Soc.* **143**, 15413–15419 (2021).
30. Visse, R. et al. Enantioselective palladium-catalyzed N-allylation of lactams. *ChemistrySelect* **3**, 5216–5219 (2018).
31. Dong, X.-Y. et al. A general asymmetric copper-catalysed Sonogashira C(sp^3)–C(sp) coupling. *Nat. Chem.* **11**, 1158–1166 (2019).
32. Wang, F.-L. et al. Mechanism-based ligand design for copper-catalysed enantioconvergent C(sp^3)–C(sp) cross-coupling of tertiary electrophiles with alkynes. *Nat. Chem.* **14**, 949–957 (2022).
33. Pollegioni, L. & Servi, S. (eds) *Unnatural Amino Acids: Methods and Protocols* (Springer, 2012).
34. Li, X.-T., Gu, Q.-S., Dong, X.-Y., Meng, X. & Liu, X.-Y. A copper catalyst with a cinchona-alkaloid-based sulfonamide ligand for asymmetric radical oxytrifluoromethylation of alkenyl oximes. *Angew. Chem. Int. Ed.* **57**, 7668–7672 (2018).
35. Vitaku, E., Smith, D. T. & Njardarson, J. T. Analysis of the structural diversity, substitution patterns, and frequency of nitrogen heterocycles among U.S. FDA approved pharmaceuticals. *J. Med. Chem.* **57**, 10257–10274 (2014).
36. Top pharmaceuticals poster. *Univ. Arizona* https://njardarson.lab.arizona.edu/content/top-pharmaceuticals-poster (2022).
37. Bansal, Y. & Silakari, O. Multifunctional compounds: smart molecules for multifactorial diseases. *Eur. J. Med. Chem.* **76**, 31–42 (2014).
38. Reddy, P. M., Babu, R. J. & Reddy, P. B. An improved process for the preparation of (*S*)-2-[[4-[(3-fluorophenyl)methoxy]phenyl]methyl]aminopropanamide and its salts. India patent IN202041019522A (2021).

Data availability

The data supporting the findings of this study are available within the paper and its Supplementary Information (experimental procedures and characterization data) and from the Cambridge Crystallographic Data Centre (https://www.ccdc.cam.ac.uk/structures; crystallographic data are available free of charge under CCDC reference numbers CCDC 2190243–2190245, 2204330, 2204331 and 2238358).

Acknowledgements Financial support from the National Key R&D Program of China (nos. 2021YFF0701604 and 2021YFF0701704), the National Natural Science Foundation of China (nos. 22025103, 92256301 and 21831002), Guangdong Innovative Program (no. 2019BT02Y335), Guangdong Innovative and Entrepreneurial Research Team Program (no. 2021ZT09C278), Guangdong Provincial Key Laboratory of Catalysis (no. 2020B121201002) and Shenzhen Science and Technology Program (nos. KQTD20210811090112004 and JCYJ20200109141001789) is acknowledged. We appreciate the assistance of SUSTech Core Research Facilities.

Author contributions J.-J.C., J.-H.F. and X.-Y.D. designed the experiments and analysed the data. J.-J.C., J.-H.F., X.-Y.D., J.-Y.Z., J.-Q.B., F.-L.W., C.L., W.-L.L., X.-Y.D. and Z.-L.L. performed the experiments. J.-R.L. performed the theoretical calculations. Q.-S.G., Z.D. and X.-Y.L. wrote the paper. X.-Y.L. conceived and supervised the project.

Competing interests The authors declare no competing interests.

Additional information

Supplementary information The online version contains supplementary material available at https://doi.org/10.1038/s41586-023-05950-8.

Correspondence and requests for materials should be addressed to Xin-Yuan Liu.

Peer review information *Nature* thanks the anonymous reviewers for their contribution to the peer review of this work.

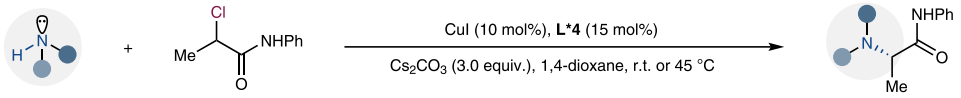

Aliphatic amine | **E1** | **57–98**

Building blocks: 1° amine scope

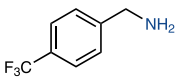

57
77%, 95% e.e.

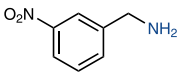

58
69%, 95% e.e.[a]

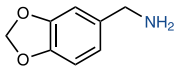

59
83%, 93% e.e.

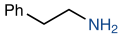

60
71%, 91% e.e.[b]

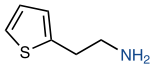

61
46%, 92% e.e.[c]

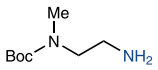

62
75%, 94% e.e.[c]

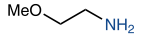

63
76%, 89% e.e.[c]

64
64%, 91% e.e.[a,c]

65
50%, 90% e.e.[c]

66
61%, 92% e.e.[a,c]

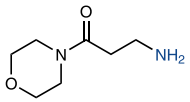

67
51%, 95% e.e.[a,c]

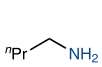

68
70%, 93% e.e.[c]

69
52%, 97% e.e.[a,c]

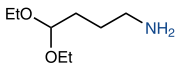

70
77%, 91% e.e.[c]

71
64%, 91% e.e.[c]

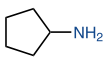

72
81%, 95% e.e.[c,d]

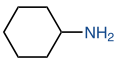

73
54%, 91% e.e.[b,d]

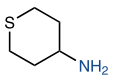

74
45%, 95% e.e.[a,b,d]

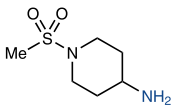

75
35%, 96% e.e.[b,d]

76
84%, 92% e.e.[b,e]

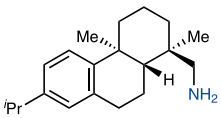

77
71%, >20:1 d.r.[b,e]

Building blocks: 2° amine scope[f]

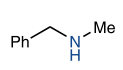

78
86%, 91% e.e.

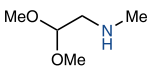

79
58%, 91% e.e.

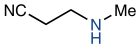

80
51%, 93% e.e.

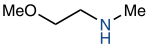

81
52%, 90% e.e.

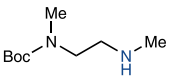

82
55%, 91% e.e.

83
78%, 93% e.e.

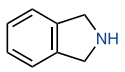

84
77%, 96% e.e.[a]

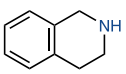

85
78%, 90% e.e.

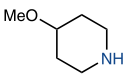

86
92%, 94% e.e.

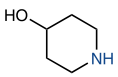

87
57%, 92% e.e.

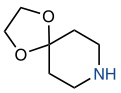

88
91%, 93% e.e.

89
99%, 93% e.e.

90
66%, 92% e.e.

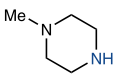

91
97%, 95% e.e.

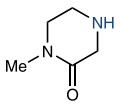

92
54%, 90% e.e.

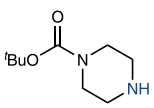

93
82%, 92% e.e.

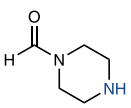

94
57%, 93% e.e.

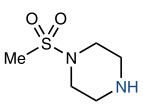

95
75%, 93% e.e.

96
71%, 94% e.e.

97
57%, 95% e.e.

98
85%, 93% e.e.[g]

Extended Data Fig. 1 | Continued scope of amines. Standard reaction conditions: amine (0.20 mmol), racemic alkyl chloride **E1** (1.5 equiv.), CuI (10 mol%), **L*4** (15 mol%) and Cs_2CO_3 (3.0 equiv.) in 1,4-dioxane (4.0 ml) under argon at 45 °C. The yields are isolated. The e.e. values are based on chiral high-performance liquid chromatography analysis. The d.r. value is based on crude ^{1}H NMR analysis. [a]Amine hydrochloride (0.20 mmol) and Cs_2CO_3 (4.0 equiv.). [b]**L*5** (15 mol%) in *N*-methyl-2-pyrrolidone/ethyl acetate (2.8 ml/1.2 ml) at r.t. [c]**L*5** (15 mol%) in *N*-methyl-2-pyrrolidone/ethyl acetate (2.4 ml/1.6 ml) at r.t. [d]**L*2** (15 mol%). [e]**L*4** (15 mol%). [f]$CuBH_4(PPh_3)_2$ (10 mol%), **L*5** (15 mol%) in *N*,*N*-dimethylformamide/cyclohexane (3.2 ml/0.80 ml) at r.t. [g]Amine dihydrochloride (0.20 mmol) and Cs_2CO_3 (5.0 equiv.).

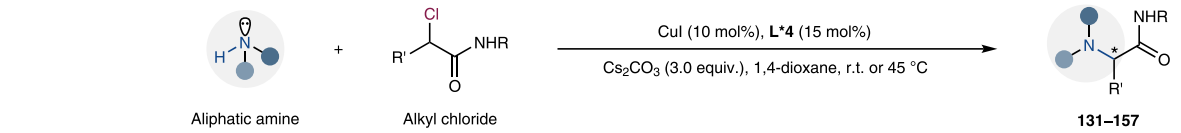

Amide R scope:

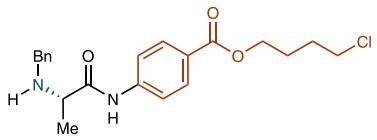

131, 89%, 90% e.e.

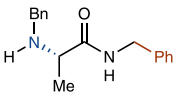

132, 56%, 82% e.e.

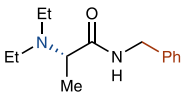

133, 63%, 84% e.e.[a]

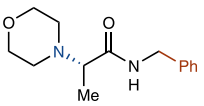

134, 67%, 94% e.e.[a]

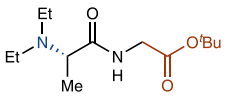

135, 78%, 98% e.e.[b] (97%, 92% e.e.)[b,c]

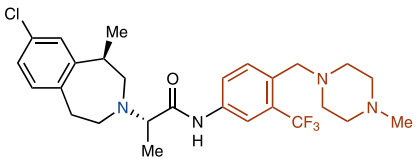

136, 76%, >20:1 d.r.[a,d]

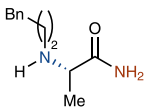

137, 41%, 93% e.e.[e]

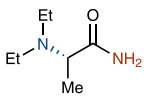

138, 87%, 88% e.e.[b]

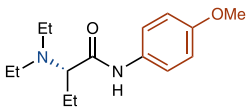

139, 72%, 97% e.e.[b]

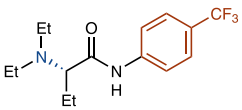

140, 56%, 95% e.e.[b]

Amide R' scope:

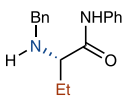

141, 85%, 92% e.e.[f]

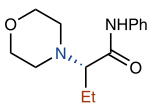

142, 99%, 96% e.e.[g]

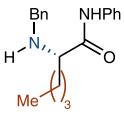

143, 98%, 90% e.e.[f]

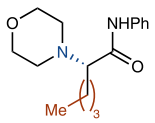

144, 99%, 95% e.e.[g]

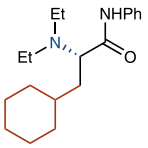

145, 89%, 95% e.e.[b]

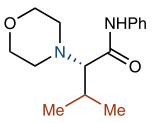

146, 36%, 87% e.e.[g]

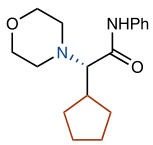

147, 57%, 81% e.e.[g]

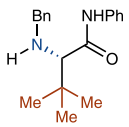

148, 79%, 87% e.e.[f]

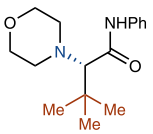

149, 74%, 87% e.e.[g]

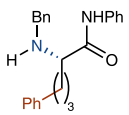

150, 88%, 85% e.e.[f]

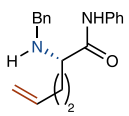

151, 78%, 92% e.e.[f]

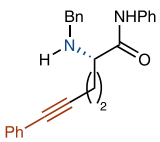

152, 51%, 94% e.e.[f]

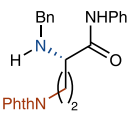

153, 58%, 88% e.e.[f]

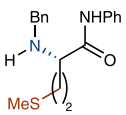

154, 75%, 85% e.e.[f]

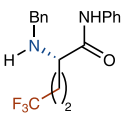

155, 79%, 97% e.e.[f]

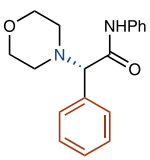

156, 89%, 94% e.e.[h]

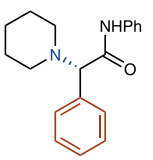

157, 85%, 94% e.e.[h]

Extended Data Fig. 2 | Continued scope of α-carbonyl alkyl chlorides. Standard reaction conditions: amine (0.20 mmol), racemic alkyl chloride (1.5 equiv.), CuI (10 mol%), **L*4** (15 mol%) and Cs_2CO_3 (3.0 equiv.) in 1,4-dioxane (4.0 ml) under argon at 45 °C. The yields are isolated. The e.e. values are based on chiral high-performance liquid chromatography analysis. The d.r. value is based on crude ^{1}H NMR analysis. [a]$CuBH_4(PPh_3)_2$ (10 mol%) and **L*5** (15 mol%) in *N*,*N*-dimethylformamide/cyclohexane (3.2 ml/0.80 ml) at r.t. [b]**L*7** (15 mol%) in benzene (4.0 ml) at 50 °C. [c]Racemic alkyl chloride (1.0 equiv.). [d]Amine hydrochloride (0.20 mmol) and Cs_2CO_3 (4.0 equiv.). [e]**L*5** (15 mol%). [f]Racemic alkyl chloride (2.0 equiv.) and **L*10** (15 mol%). [g]**L*10** (15 mol%). [h]CuSCN (10 mol%) and **L*8** (15 mol%) in tetrahydrofuran (4.0 ml) at r.t.

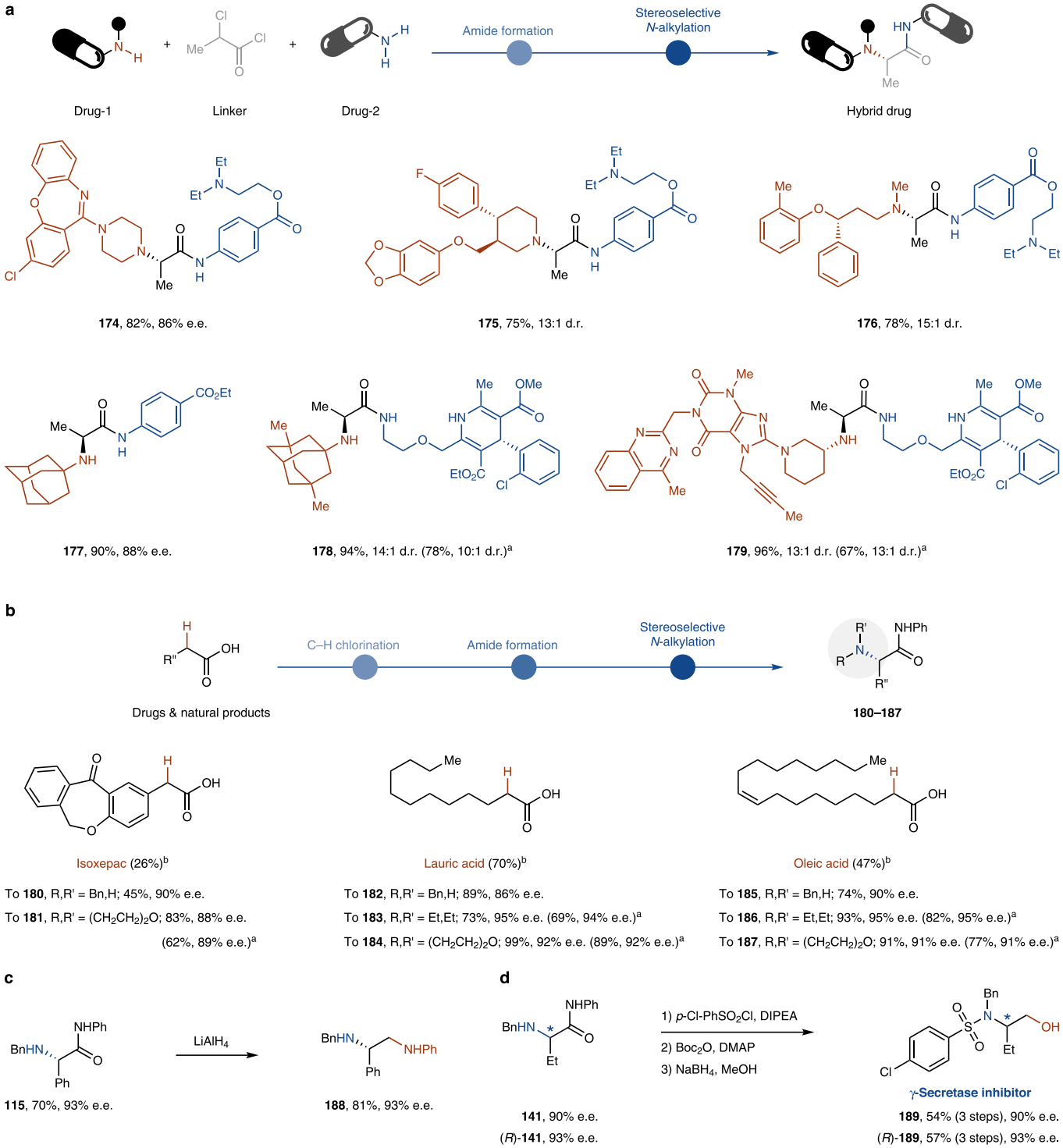

Extended Data Fig. 3 | Continued Synthetic applications in the late-stage functionalization and the preparation of complex molecules. a, Modular construction of hybrid chiral amine-containing drug molecules. **b**, Synthesis of chiral unnatural α-amino carboxamides via late-stage C(sp^3)–H functionalization of bioactive carboxylic acid molecules. **c**, Reduction of **115** to amine **188**. **d**, Conversion of carboxamide **141** to alcohol **188**. [a]Racemic alkyl chloride (1.0 equiv.). [b]Yield of α-chloro amide.

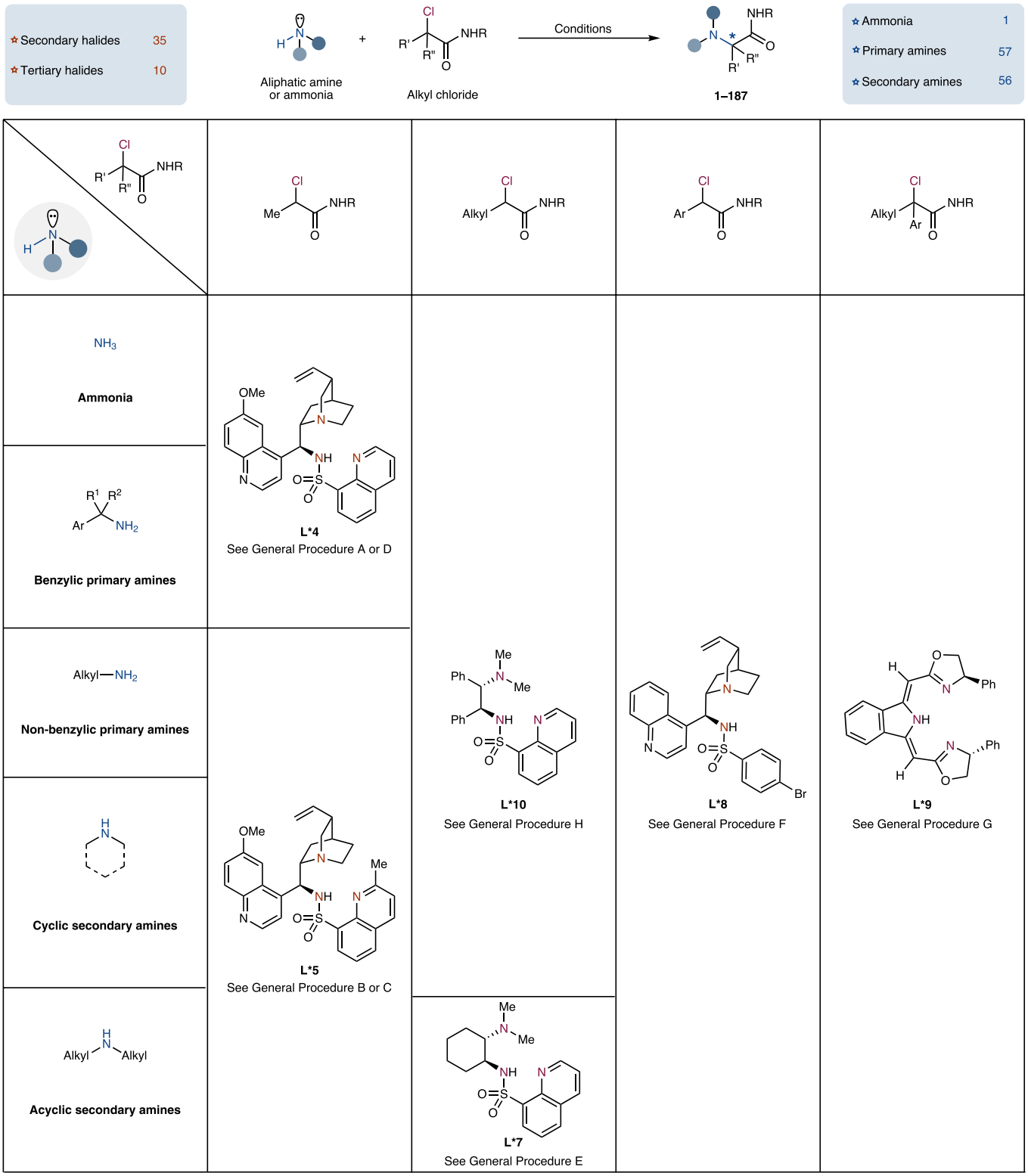

Extended Data Fig. 4 | Summary table for rapid identification of the desired chiral ligand and reaction conditions for enantioconvergent copper-catalyzed *N*-alkylation of aliphatic amines. This copper-catalyzed *N*-alkylation reaction has excellent scopes for both the alkyl halide and the amine parts; however different types of ligands were still required to achieve high enantioselectivity and reactivity. Generally speaking, alkyl halides predominantly determined the ligand choice; by contrast, amines had limited impact on the ligand choice. Specifically, small secondary alkyl chlorides such as 2-chloropropanamide required sterically congested ligand **L*4** or **L*5** for good enantioselectivity. For bulkier secondary alkyl chlorides with large α-alkyl or -aryl substituents, sterically less congested tridentate ligand **L*7** or **L*10** or bidentate ligand **L*8** performed the best. Regarding the bulkiest tertiary alkyl chlorides, planar tridentate ligand **L*9** with a likely more opened catalyst pocket was necessary for maintaining good reaction efficiency and enantioselectivity. Within the same series of alkyl chlorides, minor ligand changes such as from **L*4** or **L*7** to **L*5** or **L*10**, respectively, might deliver slightly boosted enantioselectivity.

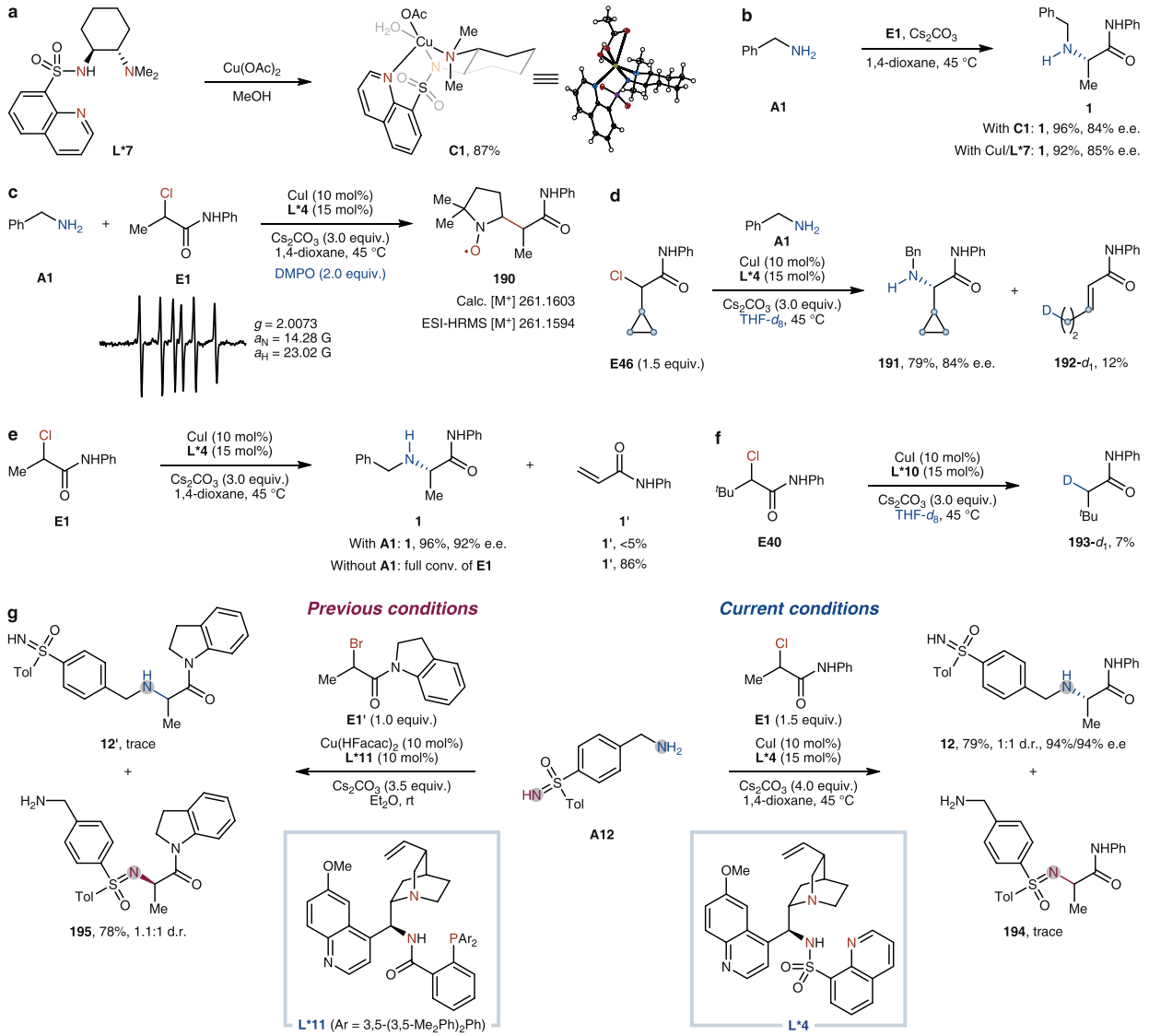

Extended Data Fig. 5 | Mechanistic experiments. a, Synthesis of copper(II) complex **C1** from **L*7** and its X-ray structure. **b**, Complex **C1** exhibited comparable catalytic activity with that in situ generated from CuI and **L*7**. **c**, EPR and HRMS experimental results indicated the formation of **190** from DMPO and the corresponding alkyl radical. **d**, In addition to the *N*-alkylation product **191**, the radical clock substrate **E46** also delivered **192**-d_1, likely via radical cyclopropane ring opening and subsequent deuterium atom abstraction from THF-d_8. **e**, In the absence of amine nucleophiles, **E1** was still completely consumed to afford the β-elimination product **1'** in high yield. **f**, By contrast, **E40** bearing no β-hydrogen atoms gave rise to **193**-d_1, likely via the formation of the corresponding alkyl radical and its subsequent deuterium atom abstraction from THF-d_8. **g**, **A12** underwent highly chemoselective amine *N*-alkylation and sulfoximine C–N cross-coupling under the current and previously reported conditions, respectively, indicating strikingly different reaction mechanisms. DCM, dichloromethane. EPR, electron paramagnetic resonance. Calc., calculated. ESI, electrospray ionization. HRMS, high-resolution mass spectroscopy. DMPO, 5,5-dimethyl-1-pyrroline *N*-oxide. THF-d_8, tetrahydrofuran. Tol, *p*-toluenyl. HFacac, hexafluoroacetylacetonate.